Silicon (2022) 14:4009–4026
https://doi.org/10.1007/s12633-021-01158-5

ORIGINAL PAPER

Experimental Investigation and Optimization of Dry Sliding Wear Test Parameters of Aluminum Based Composites

Mohammad Mohsin Khan[1] · Abhijit Dey[1] · Mohammad Irfan Hajam[1]

Received: 24 December 2020 / Accepted: 11 May 2021 / Published online: 5 June 2021

Abstract

The dry sliding wear behaviour of SiC reinforced LM13 aluminium alloy was investigated by varying the process characteristics implementing the Taguchi's Design of Experiment Methodology. Reinforcement content (0, 10, and 15 wt.% of SiC), sliding speed (2, 4, 6 m/s), applied load (10 N, 30 N, 50 N) and sliding distance (150, 300, 450 m) were selected as the independent process variables, and wear rate, frictional heating, and coefficient of friction were considered as the response characteristics followed by Taguchi's L27 orthogonal array. Pin-on-disc wear testing configuration was employed to evaluate the wear performance. ANOVA has described each process variable's percentage contribution on the performance characteristics and their significance to the study. The optimum processing condition obtained for optimal wear rates are: reinforcement of 15 wt.%, 10 N load @ 2 m/s and sliding distance of 300 m. Similarly, the optimum level of processing variables for frictional heating: Reinforcement of 0 wt.%, 10 N load @2 m/s and 300 m sliding distance and for coefficient of friction are reinforcement of 0 wt.%, 10 N load @ 2 m/s, and 300 m sliding distance. An overall optimal processing condition has been identified for all three performance characteristics by implementing Grey Relation Analysis (GRA). The confirmation experiments prove that the minimal deviation (2.8%) occurred while comparing the performance measures obtained by optimal parameter settings with the experimental data. The observation outcomes indicated that the most influential factor was applied load, followed by reinforcement, sliding speed, and sliding distance.

Keywords Sliding Wear characterization · Light metal alloy · Metal matrix composites · Stir casting · Optimization

1 Introduction

In recent years, automotive and aerospace industries prefer Aluminum Matrix Composites (AMC's) owing to their high stiffness, wear resistance, specific strength, lightness, and high damping capacity [1]. From cylinder blocks to suspension components, from gears to drive shafts, aluminium matrix composites' use gave promising results. The researchers made several attempts to correlate the microstructure and wear characteristics of industrial materials [2–12] and few studies have been focused on the sliding wear examination in order to understand the effect of different parameters like sliding speed, applied load, and sliding distance. Increased wear rates have been associated with matrix alloys compared to composites, and with increasing load, the rate of wear has been reported to rise at a faster rate [13]. Moreover, the increase in sliding speed results on rise in the temperature of the surface which ultimately increases the rate of wear.

Furthermore, the effect of the sliding speed and the applied load was proportional to the wear rate [14–16]. Rosenberger et al., and Tang et al., [17, 18] studied aluminum matrix alloy with different reinforcements like B_4C, Ti_3Al in 5–15% volume fractions and concluded that approx. 40% less wear was found in 10 wt.% than 5 wt% of B_4C under similar test conditions. Sudarshan & Surappa [19] reported that fly ash reinforced Aluminium alloy exhibits superior wear resistance compared to un-reinforced one. Also, the volume fraction and size of fly ash particles have a considerable effect on test materials' wear rate. Dixit & Khan [20] investigated the sliding wear behavior of aluminum alloy reinforced with different weight percent of Silicon carbide (SiC) and reported that the increase in SiC content increases wear resistance. Zhang et al. [21] used Al_2O_3 as reinforcement in Al alloys and concluded that composite wear resistance varies linearly with

✉ Mohammad Mohsin Khan
mohsinkhan@nitsri.ac.in

[1] Department of Mechanical Engineering, National Institute of Technology Srinagar, Srinagar, India

reinforcement weight percentage. The detailed study of each influencing parameters, their effects on performance characteristics, required surface morphologies for in-depth examinations for the effects of different parameters would requires high numbers of practical experimental examinations and therefore the number of test specimens also required to be very high. Hence, the investigation based on design of experimentation approach can be implemented to reduce the required experimental examination without compromising the featured performance characteristics analysis. Moreover, the investigation based on 'experimental design approach' is highly recommended for optimizing the processing conditions so that the measured performance characteristics would be optimum within the specified experimental domain.

Substantial studies have also been reported in past few decades, addressing the behavioral aspects of sliding wear surfaces for different engineering materials during sliding wear tests under different processing environments using a wide range of optimization approaches [22–25]. The primary objective of these studies was to examine the sliding wear behavior of the specified materials and to obtain the ranges for the selected processing variables that would threshold the performance characteristics in their optimum range [22–24]. However, this was not sufficient to accurately analyze the significance of process variables and their influences on performance characteristics of the Al-based alloys. Moreover, most of the study reported the prediction of overall optimum processing condition with in the specified domain so as to obtain the overall optimum performance measures. No findings have been reported to identify the optimal processing condition for obtaining individual optimum performance measures.

Hence, present work focuses to investigate the dry sliding wear behavior of stir cast SiC reinforced LM13 alloys based on taguchi's orthogonal array to examine the selected performance characteristics. It has provided the facility to look at the influence of the process variables on the process characteristics without going to a wide variety and range of experimental trial and also facilitated to find the optimum processing conditions which have altered the optimum responses within the specified experimental domain. Further, an optimal processing condition have been identified for each of the response characteristics and subsequently an overall optimum processing conditions have been predicted to optimize all the response characteristics based on Grey relation Analysis (GRA) approach. The influence of each process variables and their significance can be identified by ANOVA developing a second order quadratic model for each of performance measures (wear rates, frictional heating and coefficient of friction). Finally, the predicted optimal processing condition (settings of input process variables) can be validated by the experimentation and the results were compared.

2 Experimental Details

2.1 Material and Methods

Stir casting, which is quite an affordable process, was employed to manufacture the composites. An electrical furnace was used for the melting of matrix metal ingots which were melted in a graphite crucible at a temperature of 750 °C. SiC powder (50–100 μm) was adequately dried and put into a cylindrical die of 40 mm diameter and then pressed to obtain SiC pellets. These pellets were heated in a muffle furnace at 850 °C before adding to the preheated molten Al alloy. The melt was then mechanically stirred, utilizing an impeller for proper dispersion of SiC particles in the matrix alloy. The process was carried out at 750 °C. The liquid metal reinforced with particulates was poured into the preheated die into obtaining a 170 mm long cylindrical casting. Furthermore, the solidified casting is machined to obtain the specimens to wear tests. The schematic for the preparation of the test specimen is shown in Fig. 1. The chemical compositions of the casted materials are depicted in Table 1.

The Taguchi's L27 orthogonal array has been implemented to design the experimental trials so as to measure the robustness used to identify variability in a process to determine the best levels of control parameters and minimizing the effect of noise factors (uncontrollable factors) within the selected experimental domain [26]. The SN ratio is used to measure of how the response of the target/nominal value varies under different noise conditions. Depending on the goal of the experiment, there are three types of SN ratios; Larger is better, Nominal is best, Smaller is better. The procedure can be summarized as:

- Identify and evaluate quality characteristics and process parameters.
- Identify the objective function.
- Identify the number of levels and possible interactions for the process parameters
- Select an appropriate standard orthogonal array (OA).

Table 1 Materials and their composition

Material	Element Weight Percentage									
	Al	Cr	Cu	Fe	Mg	Mn	Ni	Si	Sic	Zn
LM13	*	0.1	0.6	0.25	1.7	0.15	1.5	11.8	–	0.25
LM13S10	*	0.1	0.6	0.25	1.7	0.15	1.5	11.8	5	0.25
LM13S15	*	0.1	0.6	0.25	1.7	0.15	1.5	11.8	10	0.25

*Balance

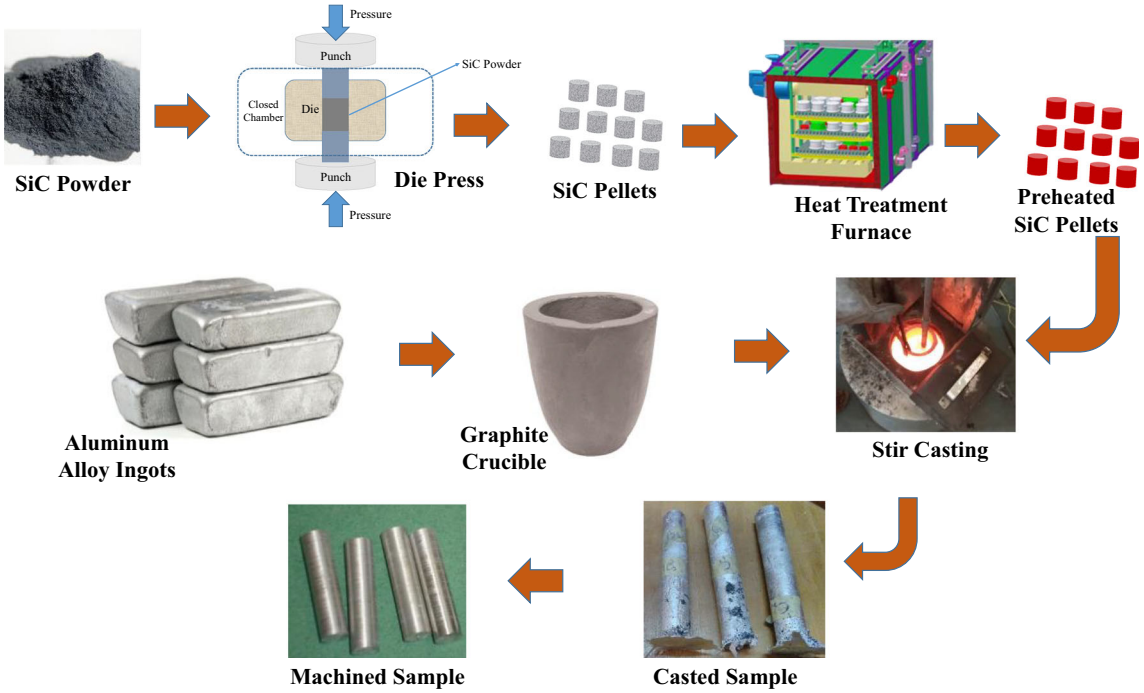

Fig. 1 Schematic illustration of the process for the preparation of test specimen

- Conduct experiments based on the run order of the orthogonal array.
- Analyze data using SN ratio and ANOVA and predict the optimum conditions
- Perform a verification experiment.

2.2 Microstructural Evaluation

Scanning electron microscopy was used to carry out the microstructural characterization of the samples. Microstructural examination was carried out on a 10 mm in diameter and 15 mm long specimen. The samples were polished using metallographic techniques and etched with Keller's reagent before examining these under the scanning electron microscope.

2.3 Wear Test

Figure 2 shows the schematic representation of a wear test. The tests were conducted as per ASTM G99–05 standard. For Pin on Disk wear testing, cylindrical specimens of length 27 mm and diameter 8 mm were used. Steel disc with a hardness of 65 HRC and surface roughness of 1–2 μm was used as the counterface material. The specimen was held by a sample holder and allowed to slide on a rotating disc. The wear test was conducted at three different loads (10 N, 30 N, and 50 N) at three different speeds (2, 4, and 6 m/s). The sample was weighted for weight loss after the interval of 150 m. Excessive vibration, strong adhesion, and abnormal noise specified the seizure of specimens, which led to the termination of the test. Frictional heating was monitored using a chromel-alumel thermocouple implanted into a 1.5 mm diameter hole at a

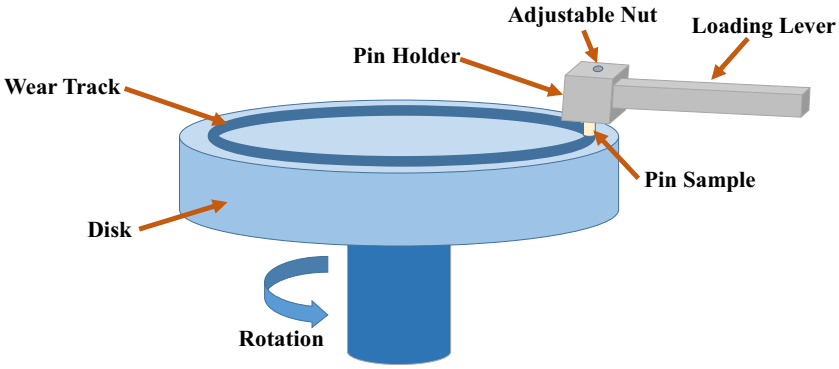

Fig. 2 Pin on Disc Wear testing arrangements

Table 2 Control Parameters and their levels

Factor	Unit	Level 1	Level 2	Level 3
Reinforcement wt.%	*	0	10	15
Sliding Speed	m/s	2	4	6
Applied Load	N	10	30	50
Sliding Distance	m	150	300	450

distance of 1.5 mm from the sliding surface. The thermocouple output is fed to a computer-based information logging system where the sample's friction heating is continually recorded during each experiment. The loads were vertically applied to the pin sample against the disc. The strain gauge result is also transferred to a computer-based data logging system that records every experiment's tangential load on the sample pin. The coefficient of friction was calculated by dividing the tangential load with the applied normal load. Wear rate was calculated using the following equation:

$$W_R = \frac{W_i - W_f}{\rho * s} \quad (1)$$

where, W_i &W_f is the initial and final weight of the specimen, ρ is the density and s is the sliding distance.

2.4 Design of Experiment

Design of experiment (DOE) is a methodology for identifying and examining all potential situations, including the various factors and variables that control an investigation. The Taguchi method is used based on DOE, which incorporates experimental and theoretical approaches to refine the most critical parameter of the response. Here, four factors (Reinforcement wt.%, applied load, sliding speed, and sliding distance) with three levels of the design was used, as presented in Table 2 to study the effect of control factors on Wear Rate, Frictional Heating and Coefficient of Friction. The degree of freedom for each control parameter is equal to one less than no. of levels of that parameter. According to the rule, the minimum no. of experimental runs should be one greater than the sum of degrees of freedom of all control parameters and their interactions. L27 Orthogonal array was used for four three-level factors, as shown in Table 3.27 experiments based on the run order generated by the Taguchi model were carried out. The responses to the model were the Wear Rate, Frictional Heating, and Coefficient of Friction. In the Orthogonal array, the columns assigned followed the order reinforcement weight percentage, sliding speed, applied load, sliding distance for the factors and responses (Wear Rate, Frictional Heating, and Coefficient of Friction) were assigned to the other columns. The purpose of

Table 3 L27 Orthogonal array of experimental layout

Expt. No.	Reinforcement (wt.%)	Sliding Speed	Applied Load	Sliding Distance
1	1	1	1	1
2	1	2	2	2
3	1	3	3	3
4	2	1	1	1
5	2	2	2	2
6	2	3	3	3
7	3	1	1	1
8	3	2	2	2
9	3	3	3	3
10	1	1	2	3
11	1	2	3	1
12	1	3	1	2
13	2	1	2	3
14	2	2	3	1
15	2	3	1	2
16	3	1	2	3
17	3	2	3	1
18	3	3	1	2
19	1	1	3	2
20	1	2	1	3
21	1	3	2	1
22	2	1	3	2
23	2	2	1	3
24	2	3	2	1
25	3	1	3	2
26	3	2	1	3
27	3	3	2	1

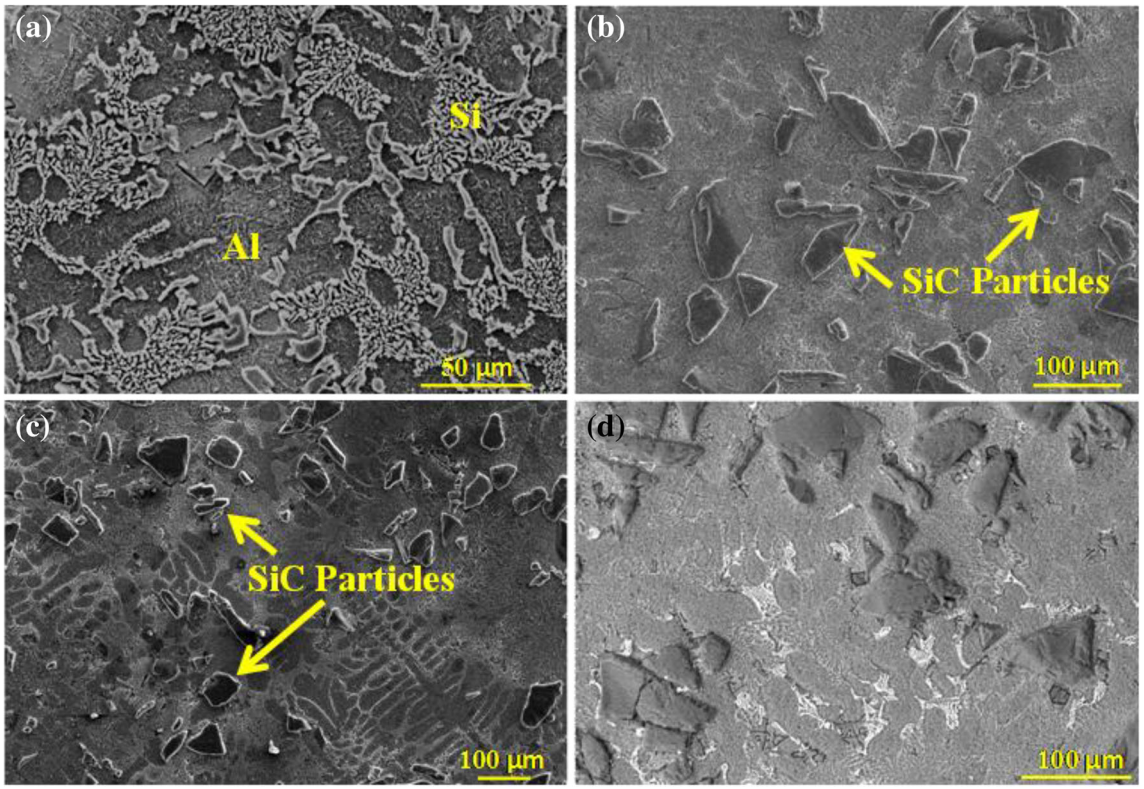

Fig. 3 SEM micrograph of the (**a**) LM13 matrix alloy showing Al and Si dendrites (**b**) 10 wt.% SiC reinforced composite (**c**) and (**d**) 15 wt.% SiC reinforced composite

the model was to minimize the Wear Rate, Frictional Heating, and Coefficient of Friction. SN ratio and Mean was calculated, and results were subjected to Analysis of Variance (ANOVA).

3 Results and Discussion

3.1 Microstructure

Figure 3a depicts the micrograph of the matrix alloy. Traces of eutectic Si, along with Al dendrites, can be observed in inter-dendritic regions. The eutectic silicon is 100 µm in length and 3–4 µm in width with an inter-dendritic arm spacing of about 35 µm. Since the eutectic structure contains both the elements, therefore solid solubility of Si in Al will be negligible. The micrograph of LM13S10 and LM13S15 composites with SiC reinforcement are shown in Fig. 3b-d. It is evident from the micrograph that the SiC particles are distributed uniformly. Instead of sitting at the inter-dendritic zone, Silicon carbide particles get trapped in the primary Al dendrites [27].

Table 4 Response Table for Signal to Noise Ratio (Smaller is better)

Level	Reinforcement wt%	Sliding Speed (m/s)	Applied Load (N)	Sliding Distance (m)
1	−31.86	−31.91	−31.20	−33.18
2	−32.75	−33.26	−33.05	−32.72
3	−34.61	−34.06	−34.98	−33.32
Delta	2.75	2.15	3.79	0.60
Rank	2	3	1	4

3.2 Signal-to-Noise Ratio Analysis

"Smaller is better" strategy, Eq. (2) is employed to analyze Signal to Noise Ratio.

$$\left(\frac{S}{N}\right)_{Smaller\ is\ better} = -10\log_{10}\left(\frac{1}{n}\sum_{i=1}^{n} Y_i^2\right) \quad (2)$$

where n is the number of observations and Y_i represents the response.

The delta value in Table 4 indicates the effect of a factor. The delta value is the difference between the highest and lowest characteristic average for a factor. The higher the variation, the higher will be the delta value, and the greater will be the significance of that parameter on the responses. The significance of the parameter determines its rank. From the rank, it is quite evident that load has a major effect on Wear Rate, Frictional Heating and Coefficient of Friction followed by the reinforcement weight percentage, sliding speed, and sliding distance.

Table 5 L27 Orthogonal array experimental layout and results

Reinforcement wt.%	Sliding Speed (m/s)	Applied Load (N)	Sliding Distance (m)	Wear Rate $X10^{-11}$ (m^3/m)	Frictional Heating (°C)	Coefficient of Friction	S/N Wear Rate	S/N Frictional Heating	S/N Coefficient of Friction
0	2	10	150	15.90	46	0.162	−24.03	−33.26	15.81
0	4	30	300	22.73	63	0.229	−27.13	−35.99	12.80
0	6	50	450	42.68	94	0.326	−32.60	−39.46	9.74
10	2	10	150	2.83	52	0.244	−9.05	−34.32	12.25
10	4	30	300	10.31	74	0.279	−20.27	−37.38	11.09
10	6	50	450	21.64	100	0.378	−26.70	−40.00	8.45
15	2	10	150	0.81	71	0.255	1.81	−37.03	11.87
15	4	30	300	2.64	93	0.338	−8.43	−39.37	9.42
15	6	50	450	4.42	139	0.391	−12.92	−42.86	8.16
0	2	30	450	14.32	58	0.163	−23.12	−35.27	15.76
0	4	50	150	45.53	77	0.249	−33.17	−37.73	12.08
0	6	10	300	21.99	57	0.295	−26.85	−35.12	10.60
10	2	30	450	1.20	65	0.239	−1.61	−36.26	12.43
10	4	50	150	29.07	92	0.349	−29.27	−39.28	9.14
10	6	10	300	12.43	66	0.259	−21.89	−36.39	11.73
15	2	30	450	0.59	89	0.278	4.61	−38.99	11.12
15	4	50	150	3.79	119	0.374	−11.57	−41.51	8.54
15	6	10	300	2.85	76	0.39	−9.10	−37.62	8.18
0	2	50	300	16.35	69	0.221	−24.27	−36.78	13.11
0	4	10	450	9.72	51	0.199	−19.76	−34.15	14.02
0	6	30	150	44.69	61	0.378	−33.00	−35.71	8.45
10	2	50	300	4.38	73	0.237	−12.82	−37.27	12.51
10	4	10	450	2.83	69	0.281	−9.05	−36.78	11.03
10	6	30	150	35.93	83	0.336	−31.11	−38.38	9.47
15	2	50	300	1.34	99	0.247	−2.56	−39.91	12.15
15	4	10	450	1.07	76	0.329	−0.57	−37.62	9.66
15	6	30	150	11.62	94	0.409	−21.31	−39.46	7.77

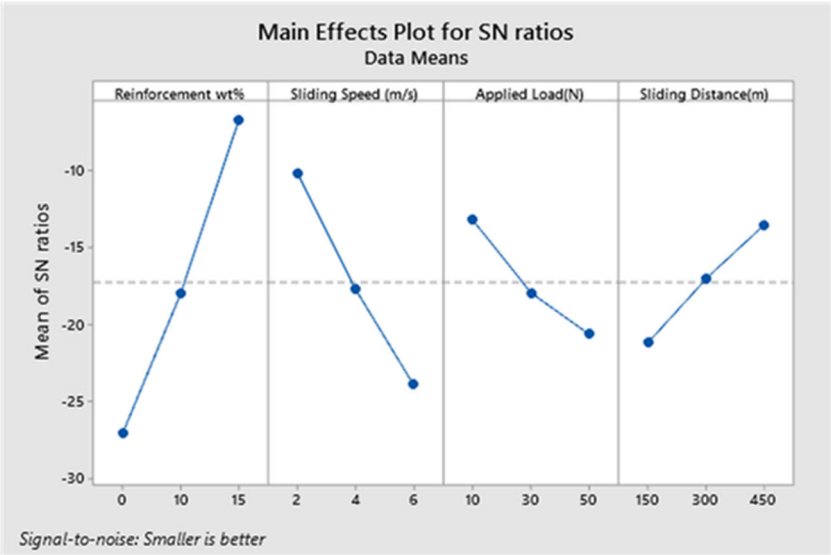

Fig. 4 Main Effects Plots for SN ratio for Wear Rate

Fig. 5 Interaction plot for SN ratio for wear rate

The sliding wear rates, frictional heating and coefficient of friction for different combinations of the variables (applied load, reinforcement weight percentage, sliding speed, and sliding distance) according to Taguchi's L27 orthogonal array (OA) are given in Table 5. MINITAB software is implemented for the DOE, and after that, subsequent analysis and plots are obtained for main effects (Fig. 4) and their interactions (Fig. 5). SN ratio plots determine the optimum level of each control parameter. From the main effects plot, the optimum condition for minimum wear rate was obtained as $A_3B_1C_1D_2$(reinforcement of 15 wt.%, 10 N load @ 2 m/s and sliding distance of 300 m). Similarly, the optimum level of processing variables for frictional heating $A_1B_1C_1D_2$(reinforcement of 0 wt.%, 10 N load @2 m/s and 300 m sliding distance) and COF $A_1B_1C_1D_2$ (reinforcement of 0 wt.%, 10 N load @ 2 m/s, and 300 m sliding distance) are obtained from main effects plot. The graph of wear rate shows the transition of wear for different parameter levels. For the composite, the wear rate shows an increase with increase in load, sliding speed and shows a decrease with rising sliding velocity. Due to presence of hard reinforcement particles, the composite shows a lower wear rate compared to aluminium alloy. The uniformly distributed SiC particles induce hardness in the composite, which in turn resists deformation of the composite and hence decreases wear rate compared to the unreinforced alloy.

3.2.1 Effects of Process Parameters on Sliding Wear

The response table (Table 6) for a signal to noise ratio depicts that the reinforcement weight percentage has the highest delta value; hence the highest significance followed by the sliding speed, sliding distance, and applied load. The wear rate decreases with the percentage increment of SiC contents owing to the enhancement of the hardness of composites with respect to the counter disc surface. Reinforcing the aluminum alloy with SiC leads to improvement in the mechanical, microstructural, and physical performance of the alloy. Also, the addition

Table 6 Response Table for Signal to Noise Ratios for Wear Rate (Smaller is better)

Level	Reinforcement wt%	Sliding Speed (m/s)	Applied Load (N)	Sliding Distance (m)
1	−27.103	−10.115	−13.163	−21.187
2	−17.974	−17.690	−17.931	−17.035
3	−6.670	−23.941	−20.653	−13.524
Delta	20.433	13.826	7.490	7.663
Rank	1	2	4	3

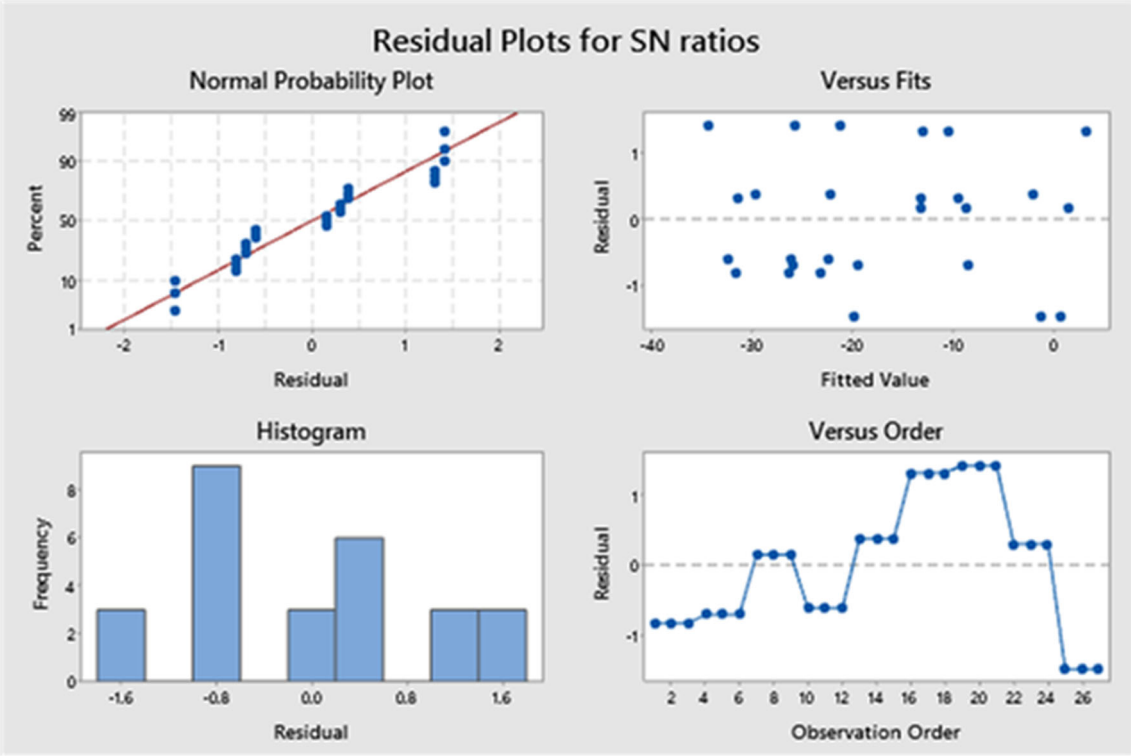

Fig. 6 Residual Plots for SN ratios for the wear rate

of SiC particles in the matrix alloy increases dislocation density and causes the deformation of the matrix.

The rate of wear is observed to be increased with the increase in sliding speed. During lower sliding speed (2 m/s), the tribo-pairs get more time to interact, which eventually enhances the interface temperature, and thereby oxidation takes place. As a result of which transition of materials occurs between the tribo-pairs. It promotes the formation of a mechanically mixed layer (MML) on the worn pin surfaces. This phenomenon can push further removal of material from the interfaces and thereby decrease the wear rates. At higher sliding speed (6 m/s), the interaction between the tribo-pairs is observed to be less and thereby the occurrence of oxidation, resulting in material transition, and after that, the chances of the formation of MML is less. It enhances the interactions of tribo-pairs which results in the occurrence of higher wear rates [28, 29].

The rate of wear is found to be increasing initially with the increase of load and subsequently, the rate of increase gets affected by the further increment in load because of the increase in contact pressure between the tribo-pairs in a linear

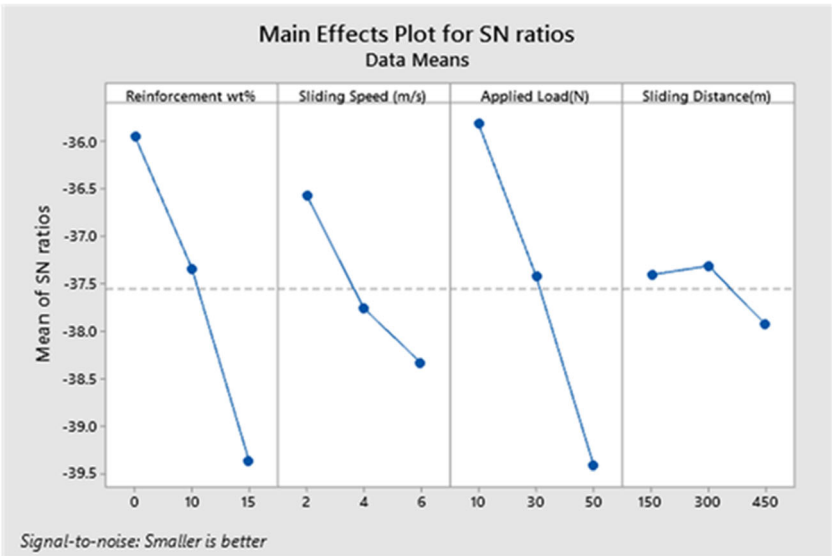

Fig. 7 Main Effects Plots for SN ratio for Frictional Heating

Table 7 Response Table for Signal to Noise Ratios for frictional heating (Smaller is better)

Level	Reinforcement wt%	Sliding Speed (m/s)	Applied Load (N)	Sliding Distance (m)
1	−35.94	−36.56	−35.81	−37.41
2	−37.34	−37.76	−37.42	−37.31
3	−39.37	−38.33	−39.42	−37.93
Delta	3.43	1.77	3.61	0.62
Rank	2	3	1	4

manner. At lower load, the pressure produced is low, resulting in lesser removal of debris material from the interfaces. Consequently, the loss of material increases in the form of debris with the increase in applied load and thereby increasing the wear rates. Hence, during higher load, a higher rate of wear is observed between the tribo-pairs resulting from greater deformation produced due to developed high pressure between the interfaces [16].

The wear plot (Fig. 4) depicts the inverse relationship of sliding distance with wear rate. During initial sliding, the delicate surface of wear out specimens comes into contact with the steel disc, resulting in the removal of soft alloy on the specimen surface; perceiving a high wear rate. As the sliding distance increases, the removal of the matrix causes the hard reinforced SiC particles to emerge on the surface. The rate of wear decreases with an increase in sliding distance due to the presence of hard SiC content in the matrix. The protrusion of reinforcing particles does not cause abrasion due to the stronger bond of the reinforcing particles to the matrix. The interacting factors have some influence on variation in the estimation of wear (Fig. 5). The interacting effect of reinforcement wt.%*sliding speed is significant to a certain extent for matrix alloy and 10 wt.% reinforced composites at 2 m/s of sliding speed while the interacting effect of reinforcement wt.%*applied load is not significant at the confidence level of 95%. Furthermore, it is worth mentioning that the consistency of the experimental data is described by the residual plots (Fig. 6). Normal probability plots for the residual indicate a data trend similar to the central one. The error bars or residuals are more concentrated in the lower error region, showing results obtained from data analysis are precise.

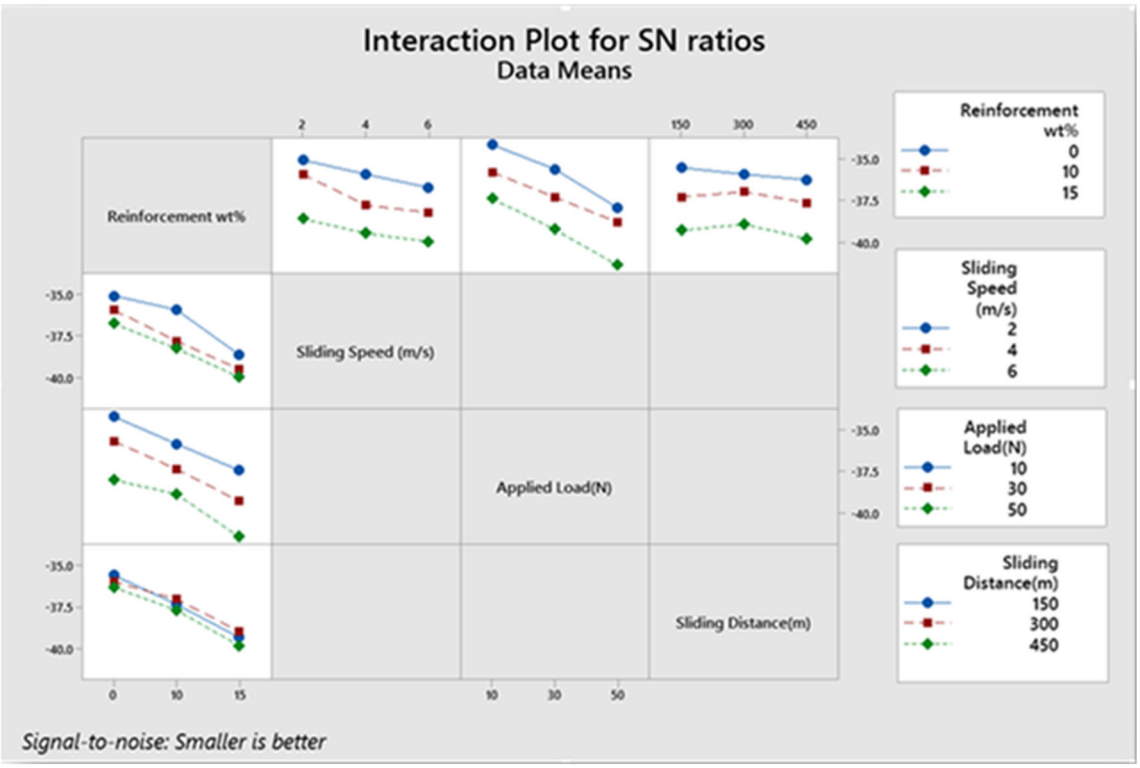

Fig. 8 Interaction plot for SN ratio for frictional heating

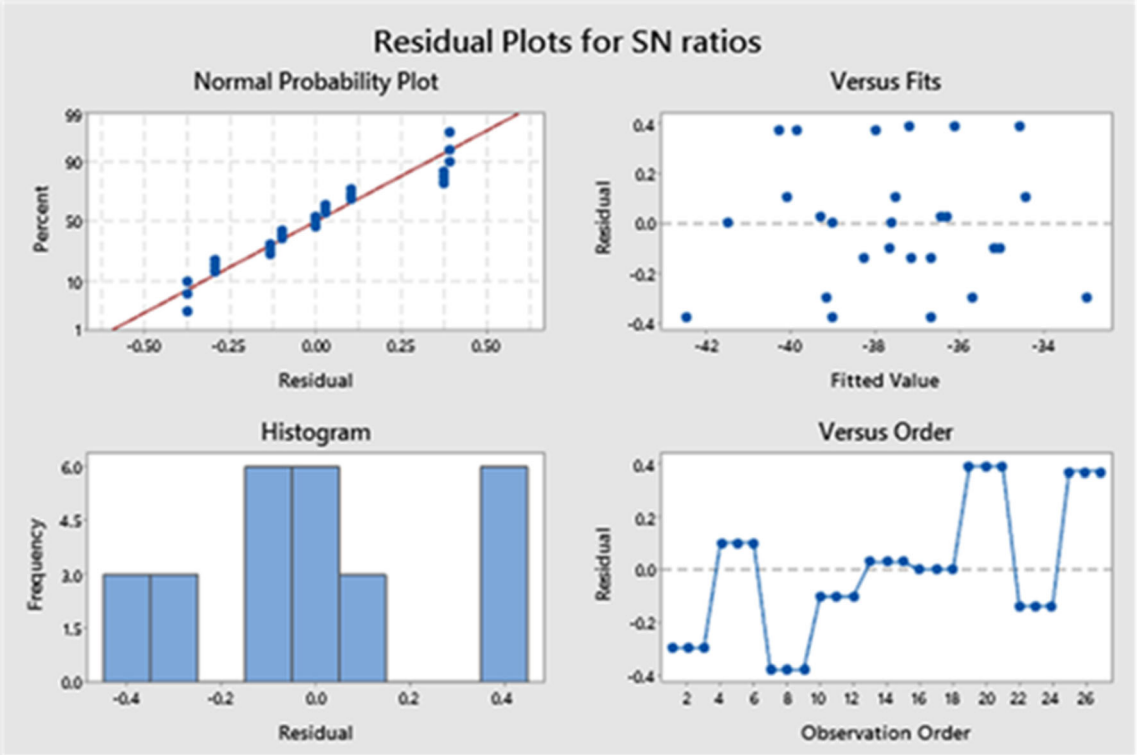

Fig. 9 Residual Plots for SN ratios for frictional heating

3.2.2 Effects of Process Parameter on Frictional Heating

From the main effects plot for SN Ratios (Fig. 7), it can be seen that reinforcement and applied load has greater significance than sliding speed and sliding distance on frictional heating. There is not much effect of sliding distance on the interfacial temperature.

The response table (Table 7) for a signal to noise ratio depicts that the applied load has the highest delta value; hence the highest significance followed by the reinforcement weight percentage, sliding speed, and sliding distance.

From the main effects plot for frictional heating (Fig. 7), it is evident that increasing the reinforcement weight percentage increases the interfacial temperature. During the initial sliding, the soft matrix particles get worn off from the surface, leaving the hard SiC particles in contact with the counterface steel disk. When hard particles under load come in contact with the hard steel surface of the disk, the temperature gets elevated.

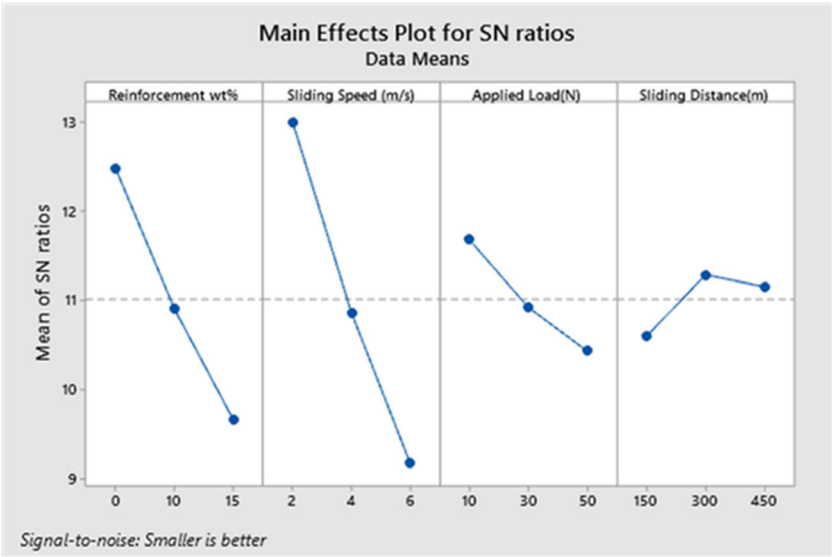

Fig. 10 Main Effects Plots for SN ratio for coefficient of friction

Table 8 Response Table for Signal to Noise Ratios (Smaller is better)

Level	Reinforcement wt.%	SlidingSpeed (m/s)	AppliedLoad (N)	SlidingDistance (m)
1	12.486	13.000	11.684	10.598
2	10.900	10.864	10.923	11.288
3	9.651	9.172	10.430	11.151
Delta	2.835	3.828	1.254	0.690
Rank	2	1	3	4

The frictional heating of all the test specimens increases with the percentage increment of SiC contents owing to the enhancement of the hardness of composites with respect to the counter disc surface. During the operation of higher wt.% SiC reinforced MMC's, the temperature is elevated and leads to a decrease in the shear strength of the pin materials. Ultimately, this effect causes significant damage in all the specimens. Reinforcing the aluminum alloy with SiC leads to improvement in the mechanical, microstructural, and physical performance of the alloy.

Figure 8 depicted that the interacting factors do not have any influence on variation in the estimation of temperature. The interacting effect of control factors is not significant at the confidence level of 95%. The residual plot for the SN ratio for frictional heating is shown in Fig. 9. A normal probability plot indicates that the data is normally distributed and the residuals follow an approximately straight line. Residuals possess constant variance as they are scattered randomly around zero in residual versus fitted values.

3.2.3 Effects of Process Parameter on the Coefficient of Friction

From the main effects plot for SN Ratios (Fig. 10), it can be seen that reinforcement and sliding speed have greater significance than load and sliding distance on the Coefficient of Friction.

The response table (Table 8) for the signal to noise ratio depicts that the sliding speed has the highest delta value; hence the highest significance, followed by the reinforcement weight percentage, load, and sliding distance, and it is worth noting that the effect of sliding distance on the Coefficient of Friction is negligible. The coefficient of friction increases proportionally with the sliding velocity due to the formation of an MML

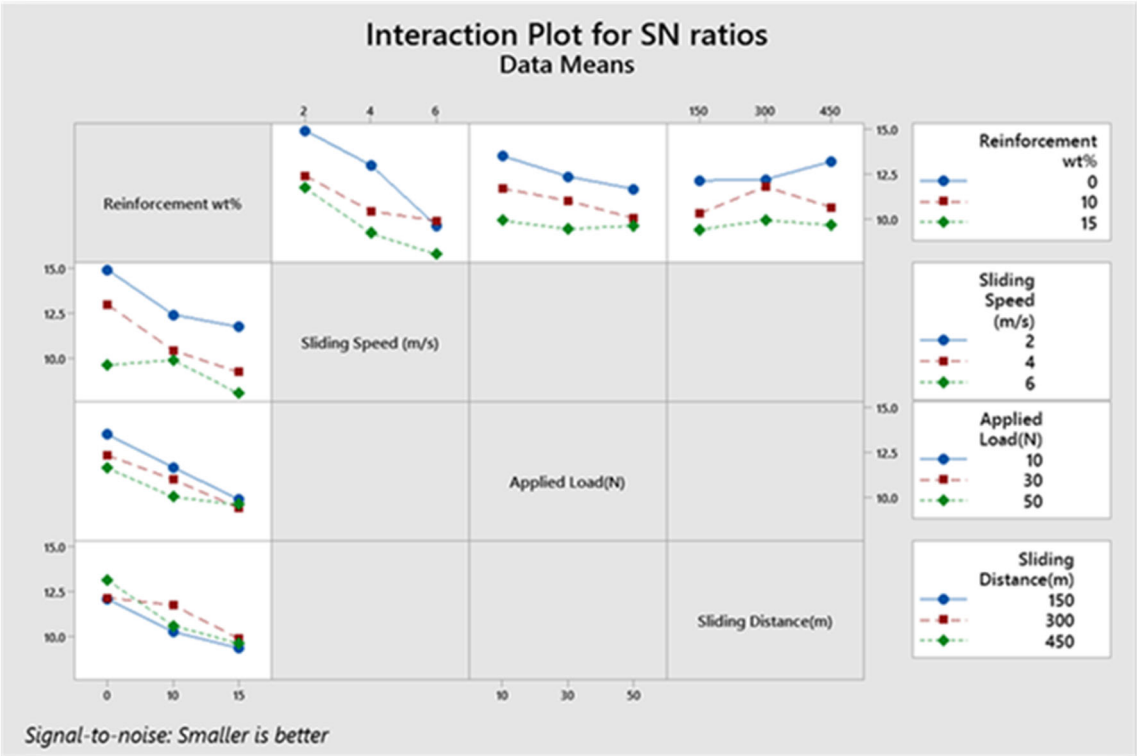

Fig. 11 Interaction plot for SN ratios for coefficient of friction

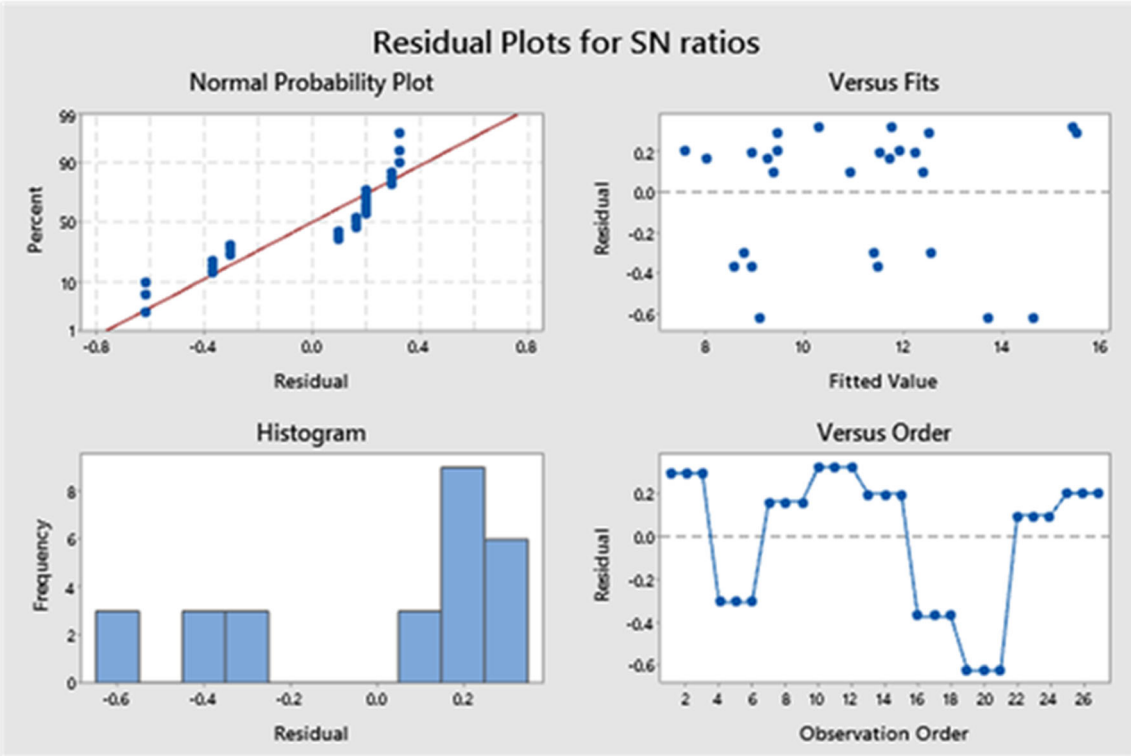

Fig. 12 Residual Plots for SN ratios for coefficient of friction

at 2 m/s. The micro-cutting phenomenon produces debris mixture that forms a compact layer when oxidized under optimum pressure and temperature. At low slide velocity (2 m/s), the interfacial heat is raised due to frictional over-heat enhancing material surface oxidation. With the velocity increasing from 2 m/s to 4 m/s, this tribo-layer produces lubricating effect on the interface thereby declining the wear rate. A similar observation was made by ZHANG et al. [30] with SiC (61%)/Cu composite, where tribo-layer resulted in 70% reduction in wear rate at intermediate velocities. At high velocity (6 m/s), this adhered layer gets removed exposing the adjacent particles over the sliding interface. This led to an increase in coefficient of friction, which in turn increased the wear rate, showing features like delamination [31].

Coefficient of Friction was observed to decrease with the increment in the distance of sliding, as observed in Fig. 10. During shorter distance (150 m), the hard reinforcement acts as the pointed asperity. This results in the phenomenon of dispersion hardening over the sliding surface. Bonding at the matrix reinforcement interface was reported to be improved, as observed by GUL et al. [32].

As indicated in Fig. 11, the interacting factors do not have any influence on variation in the estimation of the coefficient of friction. At the confidence level of 95%, the significance of the interacting effect of control factors is vacuous. The residual plots for the coefficient of friction are shown in Fig. 12. The values fall straight on line, showing the errors are normally distributed. It may be concluded that the values are within the control range, and the residual analysis shows the sufficiency of the model.

Table 9 Analysis of Variance for Wear Rate

Source	DF	Adj SS	Adj MS	F-Value	P Value	% Contribution
Reinforcement	2	2338.5	1169.23	30.90	0.000	43.72
Sliding Speed	2	1097.1	548.53	14.50	0.000	20.51
Applied Load	2	585.3	292.66	7.73	0.004	10.94
Sliding Distance	2	647.2	323.58	8.55	0.002	12.10
Error	18	681.2	37.84			
Total	26	5349.2				

Table 10 Model Summary for Wear Rate

S	R-square	R-square (adj)	R-square (pred)
6.15164	87.27%	81.61%	71.35%

Table 12 Model Summary for Frictional Heating

S	R-square	R-square (adj)	R-square (pred)
6.38768	93.76%	90.98%	85.95%

3.3 Analysis of Variance (ANOVA)

The ANOVA was performed for the 5% significance level and 95% confidence level to identify the significance of parameters and their interactions on all three responses (Tables 9, 10, 11, 12, 13 and 14). Significance level, denoted by $\alpha$is a measure of the strength of the evidence that must be present in a sample before rejecting the null hypothesis and concluding that the effect is statistically significant. *P* value, the probability that measures the evidence against the null hypothesis, if smaller than the significance level (as observed in the present study) advocates the rejection of the null hypothesis; otherwise, it accepts the null hypothesis. The percentage significance of each parameter is found out and indicated in the last column of Tables 9, 11, and 13 for wear rate, frictional heating, and coefficient of friction, respectively. From Tables 9, it is observed that reinforcement wt.% has higher significance (43.72%) on wear rate, followed by sliding speed (20.51%), sliding distance (12.1%), and applied load (10.94%). Moreover, Tables 11 delineates that the applied load has a higher significance (42.62%) on frictional heating, followed by reinforcement wt.% (38.13%), sliding speed (10.55%), and sliding distance (2.45%). Furthermore, it has been observed that the sliding speed (53.05%) has higher significance (42.62%) on the coefficient of friction, followed by reinforcement wt.% (26.51%), applied load(5.63%) and sliding distance (3%) as depicted in Tables 13.

3.4 Regression Analysis and Confirmation Experiments

The regression equations are obtained according to the sense of the parameters attained through ANOVA. The corresponding regression equations for all the three responses are given in the following equations:

$$\begin{aligned}\text{Wear Rate} = {} & 14.21 + 11.78\ \text{Reinforcement\_0} - 0.81\ \text{Reinforcement\_10} - 10.97\ \text{Reinforcement\_15} \\ & - 7.80\ \text{Sliding Speed\_2} - 0.02\ \text{Sliding Speed\_4} + 7.82\ \text{Sliding Speed\_6} \\ & - 6.38\ \text{Applied Load\_10} + 1.79\ \text{Applied Load\_30} + 4.59\ \text{Applied Load\_50} \\ & + 6.92\ \text{Sliding Distance\_150} - 3.65\ \text{Sliding Distance\_300} \\ & - 3.27\ \text{Sliding Distance\_450}\end{aligned}$$

$$\begin{aligned}\text{Frictional Heating} = {} & 78.00 - 14.00\ \text{Reinforcement\_0} - 3.11\ \text{Reinforcement\_10} + 17.11\ \text{Reinforcement\_15} \\ & - 8.89\ \text{Sliding Speed\_2} + 1.33\ \text{Sliding Speed\_4} + 7.56\ \text{Sliding Speed\_6} \\ & - 15.33\ \text{Applied Load\_10} - 2.44\ \text{Applied Load\_30} + 17.78\ \text{Applied Load\_50} \\ & - 0.78\ \text{Sliding Distance\_150} - 3.56\ \text{Sliding Distance\_300} \\ & + 4.33\ \text{Sliding Distance\_450}\end{aligned}$$

$$\begin{aligned}\text{Coefficient of Friction} = {} & 0.29019 - 0.04330\ \text{Reinforcement\_0} - 0.00107\ \text{Reinforcement\_10} \\ & + 0.04437\ \text{Reinforcement\_15} - 0.06285\ \text{Sliding Speed\_2} \\ & + 0.00170\ \text{Sliding Speed\_4} + 0.06115\ \text{Sliding Speed\_6} \\ & - 0.02196\ \text{Applied Load\_10} + 0.00415\ \text{Applied Load\_30} \\ & + 0.01781\ \text{Applied Load\_50} + 0.01604\ \text{Sliding Distance\_150} \\ & - 0.01296\ \text{Sliding Distance\_300} - 0.00307\ \text{Sliding Distance\_450}\end{aligned}$$

Table 11 Analysis of Variance for Frictional Heating

Source	DF	Adj SS	Adj MS	F-Value	P Value	% Contribution
Reinforcement	2	4486.2	2243.11	54.97	0.000	38.13
Sliding Speed	2	1240.9	620.44	15.21	0.000	10.55
Applied Load	2	5014.2	2507.11	61.45	0.000	42.62
Sliding Distance	2	288.2	144.11	3.53	0.051	2.45
Error	18	734.4	40.80			
Total	26	11,764.0				

Table 13 Analysis of Variance for the Coefficient of Friction

Source	DF	Adj SS	Adj MS	F-Value	P Value	% Contribution
Reinforcement	2	0.034600	0.017300	20.20	0.000	26.51
Sliding Speed	2	0.069231	0.034616	40.42	0.000	53.05
Applied Load	2	0.007353	0.003676	4.29	0.030	5.63
Sliding Distance	2	0.003912	0.001956	2.28	0.131	3.00
Error	18	0.015416	0.000856			
Total	26	0.130512				

3.5 Grey Relation Analysis (GRA)

The multi-response optimization using Grey relation approach is an offline quality control study contributing a practical framework to the requirement for appropriate machining condition to assessed optimum performance measures. GRA is a measurement method in grey theory which examines the uncerainity among the relations for each performance measures in the given system [33]. GRA is the advanced process of regression analysis that establishing the relationship between elements on the basis of deviation obtained among the elements [34]. The grey relational grade (GRG) is used for representing the quality illustrative for all the responses.

3.6 Implementation of GRA

Step 1: Initially, the actual values of responses are pre-processed as their obtained range were much diversified. The preprocessing of the original data is also preferred since the range and unit in a particular data concatenation may differ from others. The original sequences were converted into a comparable sequence. The characteristics of the original sequence is a "lower the better", hence the original sequence should be normalized by following Eq. 3.

$$X_I^*(K) = \frac{MAX X_I^O(K) - X_I^O(K)}{MAX X_I^O(K) - MIN\ X_I^O(K)} \tag{3}$$

However, if there is a definite goal (desired value) to be attained, then the original sequence will be normalized in the form of:

$$X_I^*(K) = 1 - \frac{\left|X_I^O(K) - X^O\right|}{MAX X_I^O(K) - X^O} \tag{4}$$

where $i = 1, \ldots, m; k = 1, \ldots, n$. m is the number of observation and n is the number of response. $X_I^O(K)$ represents the original data sequence, after data pre-processing, the sequence is designated as $X_I^*(K)$. $MAX\ X_I^O(K)$ is the largest value of $X_I^O(K)$, $MIN\ X_I^O(K)$ is the smallest value of $X_I^O(K)$ and X^O is the target value.

Step 2: Generation of grey relational coefficient (GRC) and GRG. To measure the relevancy between two systems or two sequences, the GRG is required. When only one sequence, $X_O(K)$, is obtainable as the reference sequence, and all other sequences perform as comparable

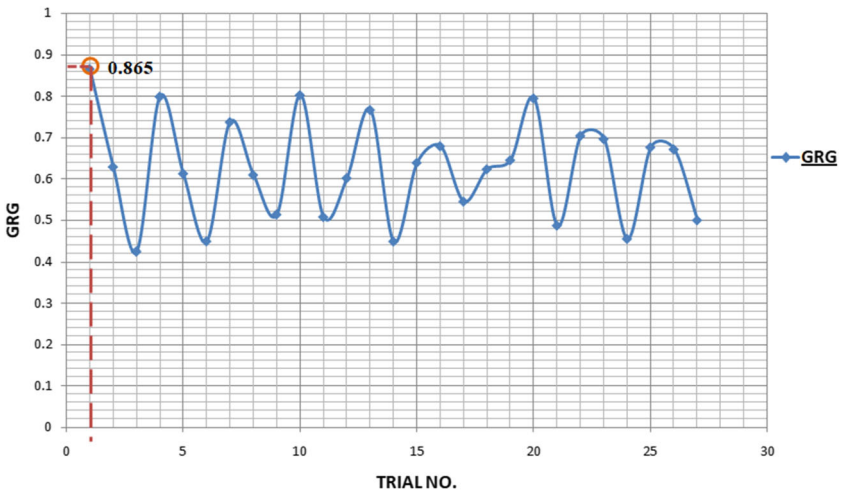

Fig. 13 Variation in GRG values during different experimental trials

Table 14 Model Summary for the Coefficient of Friction

S	R-square	R-square (adj)	R-square (pred)
0.0292653	88.19%	82.94%	73.42%

sequences which are denoted as local grey relation measurement. After data pre-processing is carried out, compute the grey relation coefficient (GRC ($\xi_i(k)$)) for the kth performance characteristics in the 'I^{th} observation to explore the correlation among the perceived and original normalized experimental results [35] using Eq. 5 [36–38].

$$\varepsilon_I(K) = \frac{\Delta_{MIN} + \varepsilon\Delta_{MAX}}{\Delta_{OI}(K) + \varepsilon\Delta_{MAX}} \tag{5}$$

Where, Δ_{OI} is the deviation sequence between reference sequence and the comparable sequence.

$$\Delta_{OI} = \left\|X_O^*(K) - X_I^*(K)\right\|$$
$$\Delta_{MIN} = \forall_{J=I}^{MIN}\forall_K^{MIN}\left\|X_O^*(K) - X_J^*(K)\right\|$$
$$\Delta_{MAX} = \forall_{J=I}^{MAX}\forall_K^{MAX}\left\|X_O^*(K) - X_J^*(K)\right\|$$

$X_O^*(K)$ is the referential sequence; $X_I^*(K)$ is the comparative sequence ζ is the distinguishing or identification coefficient. Whose value is ($\zeta \in [0,1]$), the value may be different based on the requirements of real system) chosen to Magnify the significant difference between the relational coefficients. A value of ζ is smaller and the eminent capability is greater. $\zeta = 0.5$ is generally used. After deriving the GRC value, the average of GRC values was computed using Eq. 6 to obtain the GRG. The GRG is apprehending as the single representative of the multiple quality characteristics or responses [34] Fig. 13 and Tables 15 and 16.

$$\gamma_I = \frac{1}{N}\sum_{K=1}^{N}\varepsilon_I(K) \tag{6}$$

3.7 Regression Analysis and Confirmation Experiments

The regression models have made the correlation between the responses and selected process variables such as applied load,

Table 15 Data Preprocessing and corresponding Deviation Sequences

Sl. No.	Pre-Processed Data ($X_I^*(K)$)			Deviation Seq.		
	Wear Rate (m^3/m)	Frictional Heating (°C)	Coefficient of Friction	Wear Rate (m^3/m)	Frictional Heating (°C)	Coefficient of Friction
1.	0.659	1	1	0.341	0	0
2.	0.507	0.817	0.729	0.493	0.183	0.271
3.	0.063	0.484	0.336	0.937	0.516	0.664
4.	0.95	0.935	0.668	0.05	0.065	0.332
5.	0.784	0.699	0.526	0.216	0.301	0.474
6.	0.532	0.419	0.126	0.468	0.581	0.874
7.	0.995	0.731	0.623	0.005	0.269	0.377
8.	0.954	0.495	0.287	0.046	0.505	0.713
9.	0.915	0	0.073	0.085	1	0.927
10.	0.694	0.871	0.996	0.306	0.129	0.004
11.	0	0.667	0.648	1	0.333	0.352
12.	0.524	0.882	0.462	0.476	0.118	0.538
13.	0.986	0.796	0.688	0.014	0.204	0.312
14.	0.366	0.505	0.243	0.634	0.495	0.757
15.	0.737	0.785	0.607	0.263	0.215	0.393
16.	1	0.538	0.53	0	0.462	0.47
17.	0.929	0.215	0.142	0.071	0.785	0.858
18.	0.95	0.677	0.077	0.05	0.323	0.923
19.	0.649	0.753	0.761	0.351	0.247	0.239
20.	0.797	0.946	0.85	0.203	0.054	0.15
21.	0.019	0.839	0.126	0.981	0.161	0.874
22.	0.916	0.71	0.696	0.084	0.29	0.304
23.	0.95	0.753	0.518	0.05	0.247	0.482
24.	0.214	0.602	0.296	0.786	0.398	0.704
25.	0.983	0.43	0.656	0.017	0.57	0.344
26.	0.989	0.677	0.324	0.011	0.323	0.676
27.	0.755	0.484	0	0.245	0.516	1

Table 16 Formulation of Grey relation coefficient (GRC) and Grey relation grade (GRG)

Sl. No.	GRC			GRG
	Wear Rate	Frictional Heating	Coefficient of Friction	
1.	0.595	1	1	0.865
2.	0.504	0.732	0.648	0.628
3.	0.348	0.492	0.43	0.423
4.	0.909	0.886	0.601	0.799
5.	0.698	0.624	0.514	0.612
6.	0.516	0.463	0.364	0.448
7.	0.99	0.65	0.57	0.737
8.	0.916	0.497	0.412	0.609
9.	0.854	0.333	0.35	0.513
10.	0.621	0.795	0.992	0.803
11.	0.333	0.6	0.587	0.507
12.	0.512	0.809	0.481	0.601
13.	0.974	0.71	0.616	0.766
14.	0.441	0.503	0.398	0.447
15.	0.655	0.699	0.56	0.638
16.	1	0.52	0.516	0.678
17.	0.875	0.389	0.368	0.544
18.	0.909	0.608	0.351	0.623
19.	0.588	0.669	0.677	0.645
20.	0.711	0.903	0.769	0.794
21.	0.338	0.756	0.364	0.486
22.	0.856	0.633	0.622	0.703
23.	0.909	0.669	0.509	0.696
24.	0.389	0.557	0.415	0.454
25.	0.968	0.467	0.592	0.676
26.	0.979	0.608	0.425	0.671
27.	0.671	0.492	0.333	0.499

sliding speed, traversal distance, and wt.% of reinforcement. The parameter prefixed with a positive sign shows that increasing the level of the parameter will increase the values of the response, and the parameter prefixed with negative sign implies that increasing the level of the parameter will decrease the values of the response variables. For all the three responses, the adequacy checking of the built model is performed by the validation experiment. The predicted sets of process variables are substituted in the constructed model, and obtained response for all three outputs are compared with experimental values obtained for the same set of parameters. From Table 10, Table 12 and Table 14, it is evident that R square value is higher than 85% and hence it is proved that results are more adequate for all the responses.

Attempts have been made to investigate the influence of process parameters on the overall performance measures considering all the responses as a single response indicator for the system. The combination of process parameter (Trial 1) for which the quality characteristics yielded the peak value of GRG (0.85) was selected as the initial set of the process parameter. It has been found that the hybrid GRA technique had marginally improved the quality characteristics as depicted in Fig. 14.The approach is one of its kind and observed to be fit appropriately with the actual experimentation and closest to the predicted optimal processing conditions implementing for individual responses. This experimental data set, along with the selected approach for finding optimal processing conditions, are providing a reference for database for technological improvements in industrial applications.

4 Conclusions

Several confrontations must be surmounted in order to improve the wear behavior of discontinuous particle reinforced Al alloys like fabrication processes, the influence of reinforcement, type and size of the reinforcements, etc. However, the key points derived from the present study can be summarized as:

- Hard SiC ceramic particles are successfully incorporated into the LM13 matrix alloy through improved stir casting technique.
- The hardness of the composite was gradually improved with rising content of SiC particles.
- The wear resistance of the alloy reinforced with SiC is higher than that of other alloys under severe wear conditions. This could be attributed to the high level of stability of oxide films on worn surfaces.
- Dry sliding wear behaviour of SiC reinforced composites has been analyzed through SN ratio in correlation with ANOVA and the optimum processing condition obtained for optimal wear rates are: reinforcement of 15 wt.%, 10 N load @ 2 m/s and sliding distance of 300 m. Similarly, the optimum level of processing variables for Frictional Heating: Reinforcement of 0 wt.%, 10 N load @2 m/s and 300 m sliding distance and for COF are: reinforcement of 0 wt.%, 10 N load @ 2 m/s, and 300 m sliding distance.
- The overall optimal performance characteristics obtained by the optimum processing conditions predicted by Grey Relation Analysis (GRA) and observed minimal error percentage (2.8%). which prove the approximation of implemented GRA approach along with SN ratio analysis towards identifying optimal solutions for such MCDM problems.

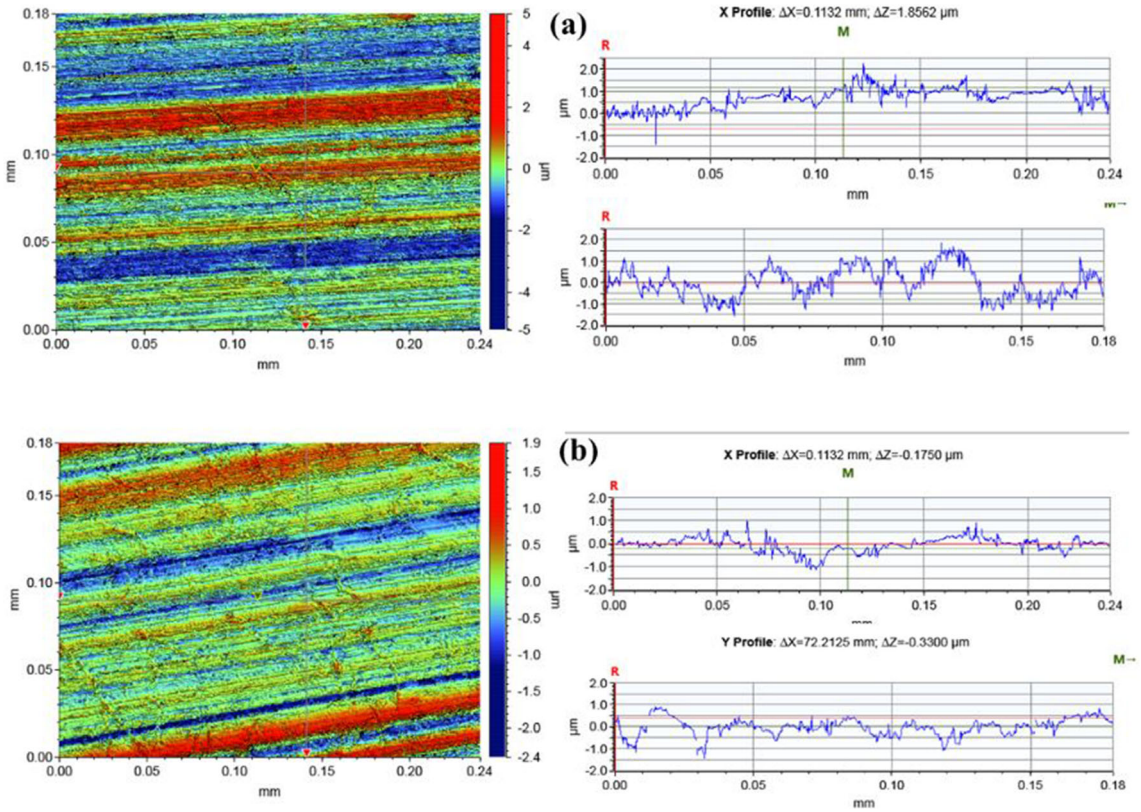

Fig. 14 2D optical images of wear out sample, ((**a**) using normal parameter settings **(b** Using optimal parameter setting predicted by GRA (crest value of GRG)

Acknowledgments The authors would like to thank Dr. Noor Zaman Khan of the Mechanical Engineering Department, National Institute of Technology, for his support in the research work.

Author Contribution Dr. Mohammad Mohsin Khan: Conception of design of study; acquisition of data, drafting the manuscript, critical revision of manuscript.

Dr. Abhijit Dey: Analysis & Interpretation of data.

Mr. Mohammad Irfan Hajam: Analysis &Interpretation of data; drafting the manuscript.

Funding No funding was received for this work.

Data Availability The data that support the findings of this study are available from the corresponding author upon reasonable request.

Declarations We confirm that any aspect of the work covered in this manuscript that has involved human patients has been conducted with the ethical approval of all relevant bodies and that such approvals are acknowledged within the manuscript. Written consent to publish potentially identifying information, such as details or the case and photographs, was obtained from the patient(s) or their legal guardian(s).

Consent to Participate All the authors listed in the manuscript are agree to participate in this research study.

Consent for Publication We confirm that the manuscript has been read and approved by all named authors. We confirm that the order of authors listed in the manuscript has been approved by all named authors.

Conflict of Interest We wish to confirm that there are no known conflicts of interest associated with this publication and there has been no significant financial support for this work that could have influenced its outcome.

References

1. Rao R, Das S (2011) Effect of SiC content and sliding speed on the wear behaviour of aluminium matrix composites. Mater Des 32(2): 1066–1071
2. Khan M, Dixit G (2017) Erosive wear response of SiCp reinforced aluminium based metal matrix composite: effects of test environments. J Mech Eng Sci 14:2401–2414
3. Khan MM, Dixit G (2017) Effects of test parameters and SiCp reinforcement on the slurry erosive wear response of Al-Si alloy. Mat Today: Proceed 4(2):3141–3149
4. Khan MM, Dixit G (2017) Comparative study on erosive wear response of SiC reinforced and fly ash reinforced aluminium based metal matrix composite. Mat Today: Proceed 4(9):10093–10098
5. Khan MM, Dey A (2021) Selection of optimal processing condition during abrasive Wear of in-situ ZA-37/TiCp composites using MCDM technique. Ceram Int
6. Khan MM, Dixit G (2018) Abrasive Wear characteristics of silicon carbide particle reinforced zinc based composite. Silicon 10(4): 1315–1327
7. Findik F (2014) Latest progress on tribological properties of industrial materials. Mater Des 57:218–244

8. Soy U, Demir A, Findik F (2011) Friction and wear behaviors of Al-SiC-B4C composites produced by pressure infiltration method. Industrial LubricatTribol 63:387–393
9. Altinkok N, Demir A, Ozsert I, Findik F (2007) Compressive behavior of Al2O3—SiC ceramic composite foams fabricated by decomposition of aluminum sulfate aqueous solution. J Compos Mater 41(11):1361–1373
10. Ozsarac U, Findik F, Durman M (2007) The wear behaviour investigation of sliding bearings with a designed testing machine. Mater Des 28(1):345–350
11. Bains, P.S., et al., Investigation of surface properties of Al–SiC composites in hybrid electrical discharge machining, in Futuristic Composites. 2018, Springer. p. 181–196
12. Bains PS, Payal H, Sidhu SS Analysis of coefficient of thermal expansion and thermal conductivity of bi-modal SiC/A356 composites fabricated via powder metallurgy route. In ASME 2017 Heat Transfer Summer Conference. 2017. Am Soc Mech EngDigit Collect
13. Lim C, Lim S, Gupta M (2003) Wear behaviour of SiCp-reinforced magnesium matrix composites. Wear 255(1–6):629–637
14. Qin Q, Zhao Y, Zhou W (2008) Dry sliding wear behavior of Mg2Si/Al composites against automobile friction material. Wear 264(7–8):654–661
15. Ramesh C et al (2010) Friction and wear behavior of Ni–P coated Si3N4 reinforced Al6061 composites. Tribol Int 43(3):623–634
16. Uyyuru R, Surappa M, Brusethaug S (2007) Tribological behavior of Al–Si–SiCp composites/automobile brake pad system under dry sliding conditions. Tribol Int 40(2):365–373
17. Rosenberger MR, Schvezov C, Forlerer E (2005) Wear of different aluminum matrix composites under conditions that generate a mechanically mixed layer. Wear 259(1–6):590–601
18. Tang F, Wu X, Ge S, Ye J, Zhu H, Hagiwara M, Schoenung JM (2008) Dry sliding friction and wear properties of B4C particulate-reinforced Al-5083 matrix composites. Wear 264(7–8):555–561
19. Surappa M (2008) Dry sliding wear of fly ash particle reinforced A356 Al composites. Wear 265(3–4):349–360
20. Dixit G, Khan MM (2014) Sliding Wear Response of an Aluminium Metal Matrix Composite: Effect of Solid Lubricant Particle Size. Jordan J Mech Industrial Eng 8(6)
21. Zhang Z, Zhang L, Mai Y-W (1997) Modeling steady wear of steel/Al2O3 Al particle reinforced composite system. Wear 211(2):147–150
22. Dey A, Bandi VR, Pandey K (2018) Wire electrical discharge machining characteristics of AA6061/cenosphere aluminium matrix composites using RSM. Mat Today: Proceed 5(1):1278–1285
23. Dey A, Debnath M, Pandey KM (2017) Analysis of effect of machining parameters during electrical discharge machining using Taguchi-based multi-objective PSO. Int J Comput Intell Appl 16(02):1750010
24. Dey A, Pandey KM (2018) Wire electrical discharge machining characteristics of AA6061/cenosphere as-cast aluminum matrix composites. Mater Manuf Process 33(12):1346–1353
25. Khan MM, Hajam MI, Mir ZA (2021) Optimizing the effect of solid lubricants on the sliding Wear behavior of SiC p reinforced cast aluminum alloy. J Bio- Tribo-Corrosion 7(1):1–17
26. Fisher, R. (1925) Statistical Methods for Research Workers Oliver and Boyd, London. Reprinted in Statistical Methods, Experimental Design and Scientific Inference., OUP, Oxford
27. Khan MM, Dixit G (2020) Evaluation of microstructure, mechanical, thermal and erosive Wear behavior of aluminum-based composites. Silicon 12(1):59–70
28. Siddesh Kumar NG, Ravindranath V, Shiva Shankar GS (2014) Dry sliding wear behavior of hybrid metal matrix composites. Int J Res Eng Technol 3(3):554–558
29. Zhang J, Alpas A (1997) Transition between mild and severe wear in aluminium alloys. Acta Mater 45(2):513–528
30. Zhang L, He XB, Qu XH, Duan BH, Lu X, Qin ML (2008) Dry sliding wear properties of high volume fraction SiCp/cu composites produced by pressureless infiltration. Wear 265(11–12):1848–1856
31. Radhika N, Raghu R (2017). Investigation on Mechanical Properties and Analysis of Dry Sliding Wear Behavior of Al LM13/AlN Metal Matrix Composite Based on Taguchi's Technique, J Tribol 139(4)
32. Gul F, Acilar M (2004) Effect of the reinforcement volume fraction on the dry sliding wear behaviour of Al–10Si/SiCp composites produced by vacuum infiltration technique. Compos Sci Technol 64(13–14):1959–1970
33. Tosun N (2006) Determination of optimum parameters for multi-performance characteristics in drilling by using grey relational analysis. Int J Adv Manuf Technol 28(5–6):450–455
34. Singh PN, Raghukandan K, Pai B (2004) Optimization by Grey relational analysis of EDM parameters on machining Al–10% SiCP composites. J Mater Process Technol 155:1658–1661
35. Li C-H, Tsai M-J (2009) Multi-objective optimization of laser cutting for flash memory modules with special shapes using grey relational analysis. Opt Laser Technol 41(5):634–642
36. Fung C-P (2003) Manufacturing process optimization for wear property of fiber-reinforced polybutylene terephthalate composites with grey relational analysis. Wear 254(3–4):298–306
37. Ho C-Y, Lin Z-C (2003) Analysis and application of grey relation and ANOVA in chemical–mechanical polishing process parameters. Int J Adv Manuf Technol 21(1):10–14
38. Lo S-P (2002) The application of an ANFIS and grey system method in turning tool-failure detection. Int J Adv Manuf Technol 19(8): 564–572